AD-A157 224 RENORMALIZATION OF AN INVERSE SCATTERING THEORY FOR INHOMOGENEOUS DIELECTRICS(U) NAVAL RESEARCH LAB WASHINGTON DC H D LADOUCEUR ET AL. 19 JUL 85 1/1

UNCLASSIFIED NRL-MR-5605 F/G 20/14 NL

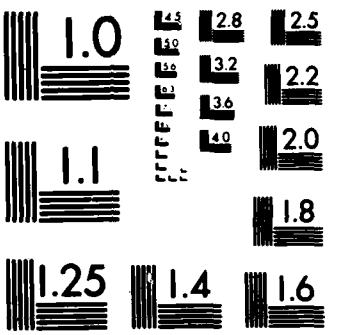

MICROCOPY RESOLUTION TEST CHART

)ARDS-1963-A

NRL Memorandum Report 5605

Renormalization of an Inverse Scattering Theory for Inhomogeneous Dielectrics

H. D. LADOUCEUR
Chemistry Division

A. K. JORDAN
Space Science Division

July 19, 1985

NAVAL RESEARCH LABORATORY
Washington, D.C.

AD A157 224

SECURITY CLASSIFICATION OF THIS PAGE

REPORT DOCUMENTATION PAGE

1a REPORT SECURITY CLASSIFICATION UNCLASSIFIED	1b RESTRICTIVE MARKINGS
2a SECURITY CLASSIFICATION AUTHORITY	3 DISTRIBUTION / AVAILABILITY OF REPORT Approved for public release; distribution unlimited.
2b DECLASSIFICATION / DOWNGRADING SCHEDULE	
4 PERFORMING ORGANIZATION REPORT NUMBER(S) NRL Memorandum Report 5605	5 MONITORING ORGANIZATION REPORT NUMBER(S)
6a NAME OF PERFORMING ORGANIZATION Naval Research Laboratory 6b OFFICE SYMBOL (If applicable)	7a. NAME OF MONITORING ORGANIZATION
6c ADDRESS (City, State, and ZIP Code) Washington, DC 20375-5000	7b. ADDRESS (City, State, and ZIP Code)
8a. NAME OF FUNDING / SPONSORING ORGANIZATION Office of Naval Research 8b. OFFICE SYMBOL (If applicable)	9. PROCUREMENT INSTRUMENT IDENTIFICATION NUMBER
8c ADDRESS (City, State, and ZIP Code) Arlington, VA 22217	10. SOURCE OF FUNDING NUMBERS PROGRAM ELEMENT NO. 61153N; PROJECT NO 41-1518-05; TASK NO. RR033-02-42; WORK UNIT ACCESSION NO 41-1518-00

11 TITLE (Include Security Classification)
Renormalization of an Inverse Scattering Theory for Inhomogeneous Dielectrics

12 PERSONAL AUTHOR(S)
Ladouceur, H.D. and Jordan, A.K.

13a. TYPE OF REPORT	13b. TIME COVERED	14 DATE OF REPORT (Year, Month, Day)	15 PAGE COUNT
Interim	FROM _____ TO _____	1985 July 19	15

16 SUPPLEMENTARY NOTATION

17 COSATI CODES			18 SUBJECT TERMS (Continue on reverse if necessary and identify by block number)
FIELD	GROUP	SUB-GROUP	Inverse scattering Dielectrics Renormalization

19 ABSTRACT (Continue on reverse if necessary and identify by block number)

Renormalized solutions are obtained for an inverse scattering problem that are equivalent to the second-order regular perturbation approximations for the exact (Gelfand-Levitan-Marchenko) theory. We have developed an inversion method for reconstructing the permittivity profiles of inhomogeneous dielectric slabs from reflection coefficient data. Solutions with increased radii of convergence are obtained. Numerical examples are demonstrated for simulated scattering data from Gaussian and parabolic profiles and homogeneous slabs.

20 DISTRIBUTION / AVAILABILITY OF ABSTRACT	21 ABSTRACT SECURITY CLASSIFICATION
☒ UNCLASSIFIED/UNLIMITED ☒ SAME AS RPT ☐ DTIC USERS	UNCLASSIFIED
22a NAME OF RESPONSIBLE INDIVIDUAL A.K. Jordan	22b TELEPHONE (Include Area Code) (202) 767-3486 22c. OFFICE SYMBOL Code 4110

DD FORM 1473, 84 MAR 83 APR edition may be used until exhausted
All other editions are obsolete

SECURITY CLASSIFICATION OF THIS PAGE

CONTENTS

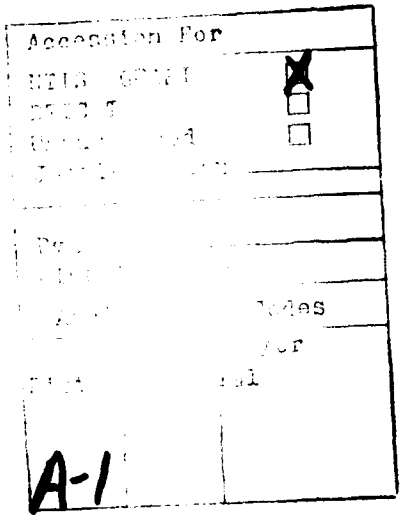

RENORMALIZATION OF AN INVERSE SCATTERING THEORY FOR INHOMOGENEOUS DIELECTRICS

INTRODUCTION

Inverse scattering theory seeks to reconstruct the unknown physical properties of an object from information contained in the scattering data. In this paper we consider the reconstruction of the dielectric profile of an inhomogeneous slab from the electromagnetic reflection coefficient. Approximate solutions to this problem are often obtained by considering a limited range of frequencies or wavelengths. For example, the wave equation for the electric field can be converted into an integral equation which is then solved by iteration. In the first iteration the Born approximation is the solution obtained by assuming small phase shifts in the scattered field. The radius of convergence for this approximation is limited to very small values of the wave-number, so that inversion methods based on this approximation will have a limited range of applicability.

In this paper we investigate a method to increase the radius of convergence of approximate solutions of inverse scattering problems by using renormalization. We base our inversion method on the exact theory that has been developed by Kay and Moses [1,2,3] from the mathematical investigations of Gelfand, Levitan and Marchenko [4,5]. The search for approximate solutions to be used for the electric field within inhomogeneous dielectric layers led us to consider the method of multiple scales [6].

By considering the continuity of the electric field and its derivative at the boundary of the slab and by using the renormalized electric field, a rapidly convergent solution is obtained that is equivalent to a second-order perturbation treatment of the exact inverse scattering theory. In the lowest order the renormalized electric field is equivalent to the WKB approximation [7]. This theory is demonstrated by numerical examples using data obtained from a numerical simulation of scattering from Gaussian and parabolic dielectric profiles and homogeneous slabs.

INVERSION THEORY

We consider the idealized physical model shown in Fig. 1. A time-harmonic plane-polarized electromagnetic wave of wave number $k = 2\pi/\lambda$

$$E_{in}(x,k) = e^{ikx}, \; i \equiv \sqrt{-1}, \quad x \leqslant -L/2, \tag{1}$$

is normally incident from the left upon an inhomogeneous dielectric slab of thickness L. The permittivity relative to free space, ϵ_r, is a function of the geometric distance x; we first demonstrate our method with ϵ_r defined by the truncated Gaussian function

$$\epsilon_r(x) = \begin{cases} Ae^{-bx^2}, & |x| \leqslant L/2 \\ 1.0, & |x| \geqslant L/2 \end{cases}, \tag{2}$$

where b is chosen to ensure continuity of ϵ_r at $|x| = L/2$. The wave amplitude $E(x,k)$ satisfies the scalar Helmholtz equation

Manuscript approved April 23, 1985.

$$\frac{d^2E(x,k)}{dx^2} + k^2\,\epsilon_r(x)\,E(x,k) = 0. \tag{3}$$

The reflected wave amplitude is

$$E_{sc}(x,k) = r(k)\,e^{-ikx}\,,\; x \leqslant -L/2 \tag{4}$$

where $r(k)$ is the complex reflection coefficient.

The electromagnetic path length s in the slab is

$$s \equiv s(x,k) = \int_{-L/2}^{x} k\,\sqrt{\epsilon_r(x')}\,dx', \tag{5}$$

which is the Liouville transformation between geometric x-space and path-length s-space [8]. The inverse problem that we consider is based upon the Helmholtz Eq. (3) with an arbitrary relative permittivity $\epsilon_r(x)$. If $\epsilon_r(x)$ is a monotonic function of x and independent of k, differential Eq. (3) can be transformed into a Schroedinger-type equation in s-space whose potential function $q(s)$ can be determined uniquely if $r(k)$ is an analytic function of k [1,2]. This theory has been well-developed, although the transformation to obtain a unique $\epsilon_r(x)$ from $q(s)$ depends on the functional form of ϵ_r, as is evident from Eq. (5), and is, in general, nontrivial.

The inversion method will, perforce, first reconstruct ϵ_r in s-space and will then make a transformation to x-space, based on *a priori* knowledge of $\epsilon_r(x)$. For notational convenience, we indicate the different functional forms of ϵ_r in these two spaces by reference to the argument x or s. The Lorentz model for the permittivity of a collection of free electrons is a simpler special case, where

$$\epsilon_r(x,k) = 1 - q(x)/k^2 \tag{6}$$

and where the profile function $q(x)$, which is the electromagnetic analogue of the quantum-mechanical potential function, is proportional to the electron density. Substitution of Eq. (6) into the Helmholtz Eq. (3) leads directly to a Schroedinger-type equation in x-space.

Referring to the Helmholtz Eq. (3), if we could assume that

$$\psi(s,k) = \left[\,\epsilon_r(x(s))\,\right]^{1/4} E(s,k) \tag{7}$$

then it would be possible to transform Eq. (3) into a Schroedinger equation of the form

$$\frac{d^2\,\psi(s,k)}{ds^2} + \left[\,k^2 - q(s)\,\right]\psi(s,k) = 0 \tag{8}$$

and where the function $q(s)$ is to be determined. This assumes we know the functional form of ϵ_r and can evaluate the integral in Eq. (5) to obtain $x(s)$ explicitly; for an inverse problem, this *a priori* information would not, in general, be available.

The Fourier transform $\Psi(s,t)$ of $\psi(s,k)$ satisfies the time-dependent wave equation

$$\frac{\partial^2}{\partial s^2}\,\Psi(s,t) - \frac{\partial^2}{\partial t^2}\,\Psi(s,t) - q(s)\,\Psi(s,t) = 0 \tag{9}$$

where t is the time variable with the velocity of light $c \equiv 1$. In free-space, $x < -L/2$, the incident plane wave, Eq. (1), and the incident wave amplitude for Eq. (8), $\psi_{in}(s,k)$, are identical; the incident plane-wave for the time-dependent Eq. (9) is represented by a unit impulse,

$$\Psi_{in}(s,t) = \delta(s - t) \tag{10}$$

which produces the reflected transient, or characteristic function,

$$R(s + t) = \frac{1}{2\pi} \int_{-\infty}^{\infty} r(k)\ e^{-ik(s + t)} dk. \tag{11}$$

Due to causality, we must have

$$R(z) = 0\ ,\ z \leqslant -L/2 \tag{12}$$

i.e., a reflected transient is not produced until the incident pulse has interacted with the inhomogeneous medium. It is possible to relate the wave amplitude $\Psi(s,t)$ in the inhomogeneous slab with the wave amplitude $\Psi_0(s,t)$ in the free-space region by the linear transformation [1]

$$\Psi(s,t) = \Psi_0(s,t) + \int_{-\infty}^{\infty} K(s,z)\ \Psi_0(z,t)\ dz, \tag{13}$$

where

$$\Psi_0(s,t) = \delta(s - t) + R(s + t). \tag{14}$$

From physical considerations we know the $\Psi(s,t)$ is a right-moving transient, so that

$$\Psi(s,t) = 0\ ,\ s > t. \tag{15}$$

Thus $K(s,t) = 0$ for $t > s$. Substituting the expression (14) in (13) and using Eq. (12) and (15) yields the integral equation

$$K(s,t) + R(s + t) + \int_{-t}^{s} K(s,z)\ R(z + t)\ dz = 0, \tag{16}$$

which is Kay's version of the Gelfand-Levitan-Marchenko integral equation of inverse scattering [3]. Substitution of the representation (13) in the wave Eq. (9) shows that the function $K(s,t)$ satisfies the same differential equation as the wave amplitude $\Psi(s,t)$ if the following conditions are imposed,

$$K(s,-s) = 0, \text{ and } 2\frac{d}{ds} K(s,s) = q(s). \tag{17}$$

If the integral Eq. (16) can be solved for the function $K(s,t)$ then the second condition in Eq. (17) yields the exact solution to this inverse scattering problem [9]. Moses [2] has obtained the second-order regular perturbation solution for $q(s)$:

$$q(s) = -2\frac{d}{ds} R(2s) + 4\left[R(2s) \right]^2. \tag{18}$$

This approximate solution of the inverse problem for a Schroedinger equation can provide a starting point to reconstruct $\epsilon_r(s)$ [10,11].

Here we go directly to the inverse problem by considering the electric fields within the slab. We note that by using the Liouville transformation (5) the differential Eq. (3) for the electric field within the slab can be expressed in terms of the electromagnetic path length s as

$$\frac{d^2E(s)}{ds^2} + g(x)\ \frac{dE(s)}{ds} + E(s) = 0, \tag{19}$$

where

$$g(x) \equiv \frac{1}{2k}\left[\epsilon_r(x)\right]^{-3/2}\frac{d\epsilon_r(x)}{dx}. \tag{20}$$

If the function $g(x)$ is small in magnitude,

$$\max|g(x)| \equiv \gamma < 1, \quad |x| \leqslant L/2 \tag{21}$$

then we can apply a regular perturbation expansion in powers of γ to eq. (19). However, such an expansion would not be uniformly valid due to the presence of secular terms in the higher-order approximations. Moreover, the explicit functional form of $g(x)$ is unknown in the inverse problem.

In performing the transformation of the Helmholtz Eq. (3) into the Schroedinger Eq. (8), it was implicitly assumed that x can be determined from eq. (5). The method of multiple scales is used to provide an effective technique for summing perturbation sequences when the explicit functional form of $\epsilon_r(x)$ is not known. Using this method, we seek an approximate solution for the electric field within the slab in the form

$$E(s(x,k),x) = E_0(s,x) + \gamma E_1(s,x) + \gamma^2 E_2(s,x) + \ldots, \tag{22}$$

where s and x are regarded as the fast and slow variables respectively. The differential equation for $E(s,x)$ can now be written through the first order in the perturbation parameter γ:

$$\gamma^0: \quad \frac{\partial}{\partial s^2}E_0(s,x) + E_0(s,x) = 0 \tag{23}$$

$$\gamma^1: \quad \frac{\partial^2 E_1(s,x)}{\partial s^2} + E_1(s,x) = -g(x)\frac{\partial E_0(s,x)}{\partial s} - \frac{2}{\sqrt{\epsilon_r(x)}}\frac{\partial^2}{\partial s \partial x}E_0(s,x).$$

The general solution of Eq. (23) is given by

$$E_0(s(x,k),x) = A_0(x)\,e^{is} + B_0(x)\,e^{-is} \tag{24}$$

Since we are only interested in right-traveling waves, we set $B_0(x) = 0$. The zero-order solution is coupled with the first-order equation for the electric field amplitude. This coupling leads to secular growth in $E_1(s,x)$, which violates energy conservation. In order to eliminate this growth the functional form of $A_0(x)$ must be determined from

$$\left\{\frac{1}{2}\left[\epsilon_r(x)\right]^{-3/2}\frac{d\epsilon_r}{dx}A_0(x) + 2\left[\epsilon_r(x)\right]^{-1/2}\frac{\partial A_0}{\partial x}\right\}\frac{\partial E_0}{\partial s} = 0, \tag{25}$$

which has the solution

$$A_0(x) = \left[\epsilon_r(x)\right]^{-1/4}, \tag{26}$$

so that the renormalized form for $E_0(s,x)$ becomes

$$E_0(s,x) = e^{is}\left[\epsilon_r(x)\right]^{-1/4}, \quad s = s(x,k). \tag{27}$$

The functional form (27) was used to transform the original Helmholtz Eq. (3) into a Schroedinger equation. The multiple scale technique demonstrates that this functional form arises from denying secular growth in the first-order correction for the electric field amplitude. This process of summing perturbation expansions to make them more uniformly valid is called renormalization [12].

Equation (19) can be converted into an integral equation by using an appropriate Green's function. Consideration of the asymptotic form of the wave solution gives an exact expression for the reflection coefficient,

$$r(k) = -\frac{i}{2} \int_{-L/2}^{L/2} [\, \epsilon_r(x) \,]^{-3/2} \frac{d\epsilon_r}{dx} \frac{d}{ds} \left\{ E(s(x,k),x) \right\} ds. \tag{28}$$

Substituting the renormalized solution (27) into Eq. (28) and application of the Fourier transform gives the approximate solution for $\epsilon_r(s)$ in s-space

$$\epsilon_r(s) = \exp\left\{ -4 \int_{-\infty}^{2s} R(z)\, dz \right\} \tag{29}$$

where the $R(z)$ term in the exponent represents the Fourier transform of the scattering data, as discussed in the next section.

A complete inversion method should also be able to obtain ϵ_r as a function of the geometric distance x, as discussed by Kay [1]. The Born approximation relates ϵ_r in x-space to the Fourier transform of $r(k)$. It is possible with our inversion method to transform from s-space to x-space if the slab thickness L is known. The WKB approximation corresponds to the first term of the perturbation solution in k-space.

Since we want to relate a discrete set of data points for $\epsilon_r(s)$ to the corresponding points within the slab in x-space, we consider the inhomogeneous region to composed of thin dielectric slabs of thickness Δ, so that $x_l = \frac{-L}{2} + (l-1)\,\Delta$, $l = 1, \ldots, N$. The number of data points N can be determined since we also know the beginning and end points of the slab in both x- and s-spaces; namely, $x_1 = -L/2$ corresponds to $s = 0$ and $x_N = L/2$ corresponds to $s = k \int_{-L/2}^{L/2} \sqrt{\epsilon_r(x')}\, dx'$, as shown in Fig. 3. In this example, N can be chosen conveniently to divide the region in s-space where ϵ_r differs from the permittivity of free space; in this example, N is approximately 50. In order to reconstruct the dielectric profile in x-space, we expand the profile in a Maclaurin series about the center of the slab

$$\epsilon_r(x) = \epsilon_r(0) + \epsilon_r'(0)\, x + \epsilon_r''(0)\, x^2/2 + \ldots . \tag{30}$$

The data points for $\epsilon_r(s)$ obtained from Eq. (29) can be transformed to the equivalent data points for $\epsilon_r(x)$ by fitting to a least squares polynomial whose coefficients can be related to Eq. (30).

GENERATION OF SCATTERING DATA

The experimental reflection data are simulated by numerical integration of the exact Riccati equation for the complex reflection coefficient, $r(k)$. The direct scattering problem is modeled by a single slab whose permittivity profile is a Gaussian function centered at the midpoint of the inhomogeneous region, as shown in Fig. 1. The magnitude of the relative permittivity ϵ_r is matched to the relative permittivity of free space at the boundaries of the slab, $|x| = L/2$. The reflection coefficient at the left face of the slab $r(k) = r(k,-L/2)$, which is used as a data point for inversion, is obtained from the solution to the Riccati equation [13]

$$\frac{dr}{dx}(x,k) = \frac{-ik}{2} \left[\epsilon_r(x) \, [\, 1 + r \,]^2 + [\, 1 - r \,]^2 \right], \quad |x| \leq \frac{L}{2} \tag{31}$$

with the boundary condition $r(k,+L/2) = 0$. The reflection coefficient $r(k)$ is calculated at discrete points x_l through the slab for each value of wavenumber k.

We use a fifth-order Runge-Kutta method with 500 increments in x to compute the complex reflection coefficients, $r(k)$, at discrete wavenumbers, $k_p = (1 - p)\,\delta$, $p = 1, \ldots, M$ (in our case $M = 256$ points were used for $k = 0$ to 25, so that the increment $\delta = 0.098$). The modulus of $r(k)$ is shown in Fig. 2 for a typical set of parameters.

For use in the inversion method, this set of reflection data (31) is then represented by a complex Fourier series,

$$r(k_p) = \frac{a_0}{2} + \sum_{m=1}^{M-2} a_m \cos(\phi_m) - ib_m \sin(\phi_m) + \frac{1}{2} a_M \cos(\pi k_p) \tag{32}$$

where $\phi_m = mk_p\pi/p$, $M = 256$ and P is the half-period of the reflection coefficient. We note that our inversion algorithm assumes $r(k)$ is periodic; as shown in Fig. 2, $P = 25$, approximately. The real part of the reflection coefficient is represented by a truncated cosine series whose coefficients are determined by requiring that the data points collocate with the series at the appropriate wavenumbers; the imaginary part of the reflection data is represented by a sine series, so the $r^*(k) = r(-k)$, k real. This continuous representation of the complex reflection coefficient enables interpolation and accurate numerical determination of the minima and maxima of $r(k)$. Moreover, the Fourier representation enables an analytic evaluation of the function $R(s)$, which is needed for the solution of the integral Eq. (16).

DISCUSSION OF RESULTS

We have demonstrated an inversion method for scattering data from a smooth dielectric profile. The scattering data of Fig. 2 were used in our inversion method to reconstruct the permittivity profile of Fig. 3. Table 1 compares the reconstructed results with several known Gaussian profiles; the parameters A, b were obtained by a regression analysis on Gaussian profiles in order to test the accuracy of this inversion method for increasing gradients in the dielectric inhomogeneity. This inhomogeneity is measured by the parameter γ, which can be shown from Eq. (19) to be equal to $b/2$. As expected, good agreement was obtained for smaller values of b and poorer agreement as b was increased. The correlation coefficient ρ tests the validity of the regression model; $\rho = 1$ indicates that the reconstructed profile agrees perfectly with the model profile.

Table 2 tests the accuracy of our method when applied to three different profiles: Gaussian, parabola, and homogeneous slab. Simulated numerical scattering data were generated by solving for each of these profiles, as characterized by equivalent A and b parameters. The inversion method was then applied to the three sets of data and profiles of ϵ_r were obtained in s-space and in x-space. By assuming that the unknown profile for $\epsilon_r(x)$ can be developed as a series of the form (30), the coefficients of the least-squares polynomial can be related to the parameters A, b of an assumed Gaussian, parabolic, or homogeneous slab model. A regression analysis with the three model profiles was used to compare the profile parameters A, b; the correlation coefficients ρ are also shown in Table 2. We note that the b parameters for the parabola and the homogeneous slab do not ensure continuity of ϵ_r at $|x| = \frac{L}{2}$. For example, the approximation for the Gaussian profile is written

$$\epsilon_r(x) \approx A(1 - bx^2). \tag{33}$$

The element along the diagonal show results due to "good guesses", i.e., the least-square analysis compared the reconstructed profile with the same model profile that was used in the direct calculation of the reflection data. The off-diagonal elements shows results comparing "wrong" regression models with different direct models. Note that this matrix is not symmetric.

From these results we see that, to second order, it is not clear whether the Gaussian or parabola is the better fit; the homogeneous slab is clearly a poor fit. The correlation coefficients for the regression

analysis for the homogeneous slab have not been display since the least-squares fit is a simple arithmetic average, so the correlation coefficient cannot be defined. The qualitative features of the slab can be reconstructured by the inversion algorithm, but the magnitude of ϵ_r is too large by 20-30%. This is expected since the homogeneous slab presents a sharp discontinuity that violates condition (21) for convergence of the perturbation series. We conjecture that our inversion method can be extended to discontinuities and steep gradients by boundary-layer theory.

The results of Table 1 show that the renormalized inversion theory has a larger radius of convergence than the Born approximation. Our inversion method also includes phase information that is neglected in the Born approximation [14],

$$(kL)\ (\epsilon_r(x) - 1) << 1 \quad . \tag{34}$$

We note that for $L = 2.0$ and $A = 1.80$, as used in our examples, the Born approximation is not valid for wavenumbers greater than 0.60 in Fig. 2. Profiles reconstructed with the Born approximation over a range of k-space of 0 to 25 were in complete disagreement with the known profiles. Renormalization has extended the radius of convergence in k-space by two orders of magnitude. The results of Table 2 suggest that the regression analysis can be extended to higher orders to consider many different model profiles. Extensions of the inversion theory to include dielectric absorption and scattering at oblique incidence would require generalizing the solution of the integral Eq. (16).

ACKNOWLEDGMENTS

The first author acknowledges support from Lt. Cdr. W. R. Schmidt of the Office of Naval Research and the second author from the 6.1 Core Research Program of the Naval Research Laboratory.

REFERENCES

1. Kay, I., "The Inverse Scattering Problem," Report No. EM-74 (Institute of Mathematical Sciences, New York University, 1955).

2. Moses, H. E., "Calculation of the Scattering Potential from Reflection Coefficients," Phys. Rev. **102**, 559-567 (1956).

3. Kay, I. and Moses, H. E., *Inverse Scattering Papers: 1955-1963* (Math Sci Press, Brookline, Mass., 1982).

4. Gelfand, I. M., and Levitan, B. M., "On the Determination of a differential equation by its spectral function," Translations of the American Mathematical Society, Series 2, **1**, 253 (1955).

5. Marchenko, V. A., "Concerning the theory of a differential operator of second order," Dokl. Akad. Nauk SSSR **72**, 457 (1950).

6. Nayfeh, M., *Perturbation Methods* (John Wiley & Sons, New York, 1973), 315.

7. Bremmer, H., "The W.K.B. approximation as the first term of a geometrical-optical series," Comm. Pure Appl. Math **3**, S169-S179 (1951).

8. Nayfeh, M., *ibid*, 315.

9. Jordan, A. K., "Inverse scattering theory: exact and approximate solutions," (*Mathematical Methods and Applications of Scattering Theory*, ed. by J. A. DeSanto, *et al*, Springer-Verlag, New York, 1980), 318-326.

10. Hirsch, J., "An analytic solution to the synthesis problem for dielectric thin-film layers," Optica Acta **26**, 1273-1279 (1979).

11. Kaiser, H., and Kaiser, H. C., "Mathematical methods in the synthesis and identification of thin-film systems: errata," Appl. Opt. **20**, 1043-1049 (1981).

12. Nayfeh, M., *ibid.*, 367.

13. Barrar, R. B., and Redheffer, R. M., "On nonuniform dielectric media," IEEE Trans. Antennas & Propagation **AP-7**, 101-107 (1955).

14. van de Hulst, H. C., *Light Scattering by Small Particles* (John Wiley & Sons, Inc., New York, 1957) 132.

Table 1 — Comparison of Reconstructed Profiles with Input Gaussian Profiles

Input parameters		Reconstructed parameters		
A	b	A	b	ρ
1.50	0.41	1.59	0.41	0.99
1.80	0.59	1.94	0.60	0.97
4.00	1.39	4.70	1.25	0.95
6.00	1.79	7.19	1.55	0.95
8.00	2.08	9.54	1.59	0.94
10.00	2.30	11.54	1.87	0.92

Table 2 — Comparison of Inversion Results for Parameters A, b for Gaussian and Parabolic Profiles and Homogeneous Slabs. Input Gaussian Profile Parameters: $A = 1.80, b = 0.59, L = 2.0$

Direct Model	Regression Model		
	Gaussian	Parabola	Slab
Gaussian	$A = 1.94$ $b = 0.60$ $\rho = 0.97$	$A = 1.92$ $b = 0.47$ $\rho = 0.96$	$A = 1.60$ $b \equiv 0$
Parabola	$A = 1.64$ $b = 0.71$ $\rho = 0.96$	$A = 1.61$ $b = 0.53$ $\rho = 0.97$	$A = 1.31$ $b \equiv 0$
Slab	$A = 3.40$ $b = 0.43$ $\rho = 0.43$	$A = 3.35$ $b = 0.31$ $\rho = 0.43$	$A = 2.98$ $b \equiv 0$

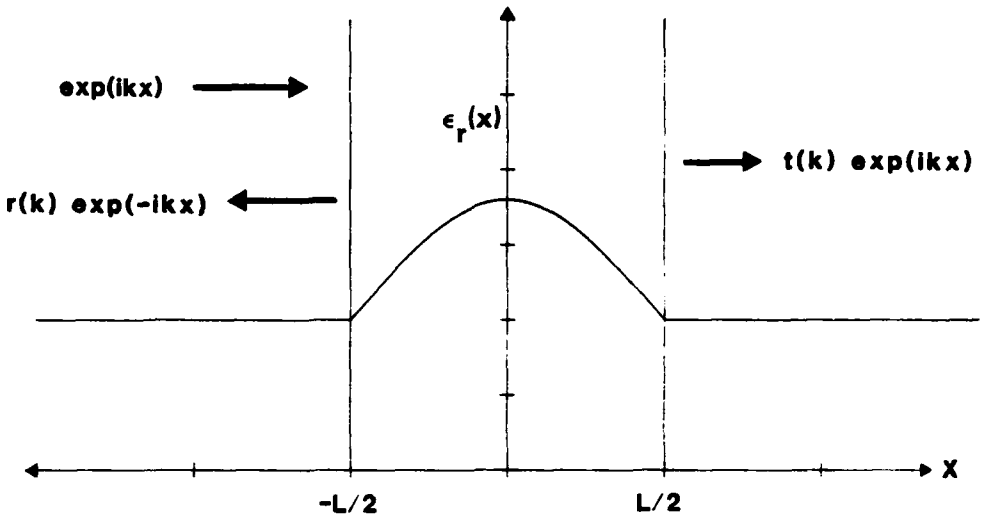

Fig. 1 — Physical model for electromagnetic reflection from an inhomogeneous dielectric slab. The slab width is L, the permittivity $\epsilon_r(x)$ is a Gaussian function $\epsilon_r(x) = Ae^{-bx^2}$ and the reflection coefficient is $r(k)$.

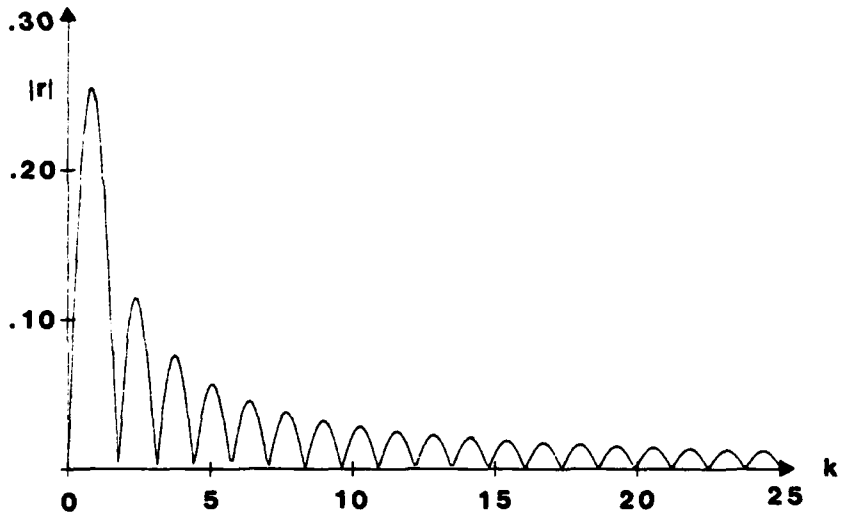

Fig. 2 — Simulated reflection data to be inverted to obtain the profile of permittivity ϵ_r. Reflection coefficient $r(k)$ data given for 256 discrete values of k. In this example, $A = 1.80$ and $b = 0.59$. The Born approximation is valid for $k \leqslant 0.6$.

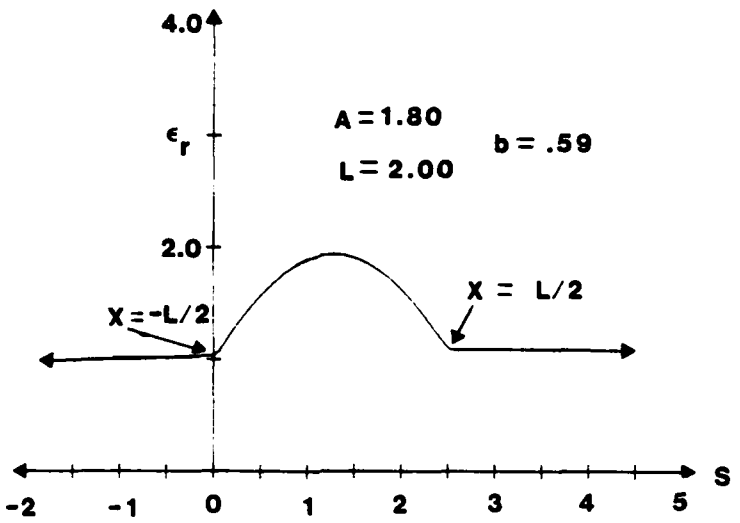

Fig. 3 — Profile of permittivity ϵ_r plotted as a function of path length s. This is a plot of approximately 130 values (511/4) obtained by applying the renormalized inversion theory to the data points of Fig. 2. Limits of slab in x-space are indicated.

END

FILMED

9-85

DTIC